Sen A *et al.* (2025)
Notulae Botanicae Horti Agrobotanici Cluj-Napoca
Volume 53, Issue 1, Article number 14218
DOI:10.15835/nbha53114218
Research Article

Biochemical and Raman spectroscopic insights into plant-mold interactions

Ayse SEN[1]*, Muhammad AHMED[2], Omar DARKAZANLI[3], Duygu GOKSAY-KADAIFCILER[4], Feyza GUZELCIMEN[5]

[1]*Istanbul University, Faculty of Science, Department of Biology, 34134, Istanbul, Türkiye; senayse@istanbul.edu.tr (*corresponding author)*
[2]*Istanbul University, Graduate School of Engineering and Science, 34116, Istanbul, Türkiye; ahmadasab93@gmail.com*
[3]*Technical University of Munich (TUM Department of Radiation Oncology and Radiotherapy), Ismaninger Str. 22, 81675 München, Germany; omar.darkazanli92@gmail.com*
[4]*Istanbul University, Faculty of Science, Department of Biology, Basic and Industrial Microbiology Section, 34134 Istanbul, Türkiye; dgoksay@istanbul.edu.tr*
[5]*Istanbul University, Faculty of Science, Department of Physics, 34134, Istanbul, Türkiye; feyzag@istanbul.edu.tr*

Abstract

Plants continuously interact with diverse biotic and abiotic factors in their environment, and understanding these intricate ecological relationships is crucial for advancing sustainable agriculture and biodiversity conservation. This study investigates the interactions between wheat plants and mold contaminants in *in vitro* cultures using Raman Spectroscopy (RS) and biochemical analyses, offering a novel approach to understanding plant responses at a molecular level. Conventional culturing methods identified *Aspergillus versicolor*, *Penicillium* sp., and *Nigrospora* sp. as the primary mold strains present in the cultures. Biochemical assays revealed that mold contamination led to a marked decrease in chlorophyll and carotenoid contents, along with an increase in thiobarbituric acid reactive substances (TBARS), indicating heightened oxidative stress. Antioxidant enzyme activities, including superoxide dismutase (SOD), peroxidase (POX), and catalase (CAT), were significantly elevated, though proline levels remained unchanged. Raman Spectroscopy further uncovered profound metabolomic shifts, particularly in carotenoid-related peaks, signalling impaired photosynthetic function. Additionally, RS detected increased carbohydrate-associated bands, suggesting that carbohydrate-derived osmolytes may play a more pivotal role than proline in maintaining cellular integrity under mold stress. To validate these findings, advanced multivariate techniques such as Principal Component Analysis (PCA) and Linear Discriminant Analysis (LDA) were employed, achieving high accuracy in distinguishing mold-infected samples from controls. These results highlight the potential of RS as a rapid, non-invasive diagnostic tool for plant health monitoring, offering significant advantages over traditional methods. This approach not only advances our understanding of plant-microbe interactions but also offers practical applications for enhancing agricultural productivity and sustainability in the face of global food security challenges.

Keywords: metabolome analysis; mold contaminations; oxidative stress in plants; plant tissue culture; Raman spectroscopy; wheat

Received: 21 Oct 2024. Received in revised form: 10 Jan 2025. Accepted: 17 Feb 2025. Published online: 26 Feb 2025.
From Volume 49, Issue 1, 2021, Notulae Botanicae Horti Agrobotanici Cluj-Napoca journal uses article numbers in place of the traditional method of continuous pagination through the volume. The journal will continue to appear quarterly, as before, with four annual numbers.

Introduction

Plants engage in complex interactions with their environment and other organisms (Beck *et al*., 2018). These relationships, with both living organisms and physical aspects of their surroundings, are crucial for plant survival and growth (Zhang *et al*., 2020). The intricate nature of these ecological interactions, constantly changing and adapting, has been a subject of intense scientific study (Bever *et al*., 1997). However, dissecting and understanding these multifaceted interactions in a simplified way remains a significant challenge (Whitham *et al*., 2010). In response, advances and applications in plant tissue culture techniques offer innovative solutions, providing new avenues to explore and overcome the obstacles presented in studying plant-environment interactions (Hussain *et al*., 2012). The complexity of ecological interactions stems from the multitude of biotic and abiotic factors influencing plant responses. For instance, the interaction between plants and mycorrhizal fungi can enhance nutrient uptake under certain soil conditions but can become parasitic under others (Smith and Read, 2010). Predicting these outcomes is challenging due to the dynamic nature of ecosystems (Whitham *et al*., 2010). Plant tissue culture methods offer controlled environments to isolate and study these interactions, free from external variability (Hussain *et al*., 2012). However, researchers face challenges such as maintaining sterile conditions, replicating natural environmental stresses, and ensuring the reproducibility of results (Bhojwani and Razdan, 1996; Leifert and Woodward, 1998). Methodological hurdles include accurately simulating field conditions and scaling findings to practical agricultural applications (Bhojwani and Razdan, 1996).

Culturing plant cells, plant parts, or organs in laboratories requires significant effort, from media preparation and cell transfer to regular maintenance. Contaminated cultures can lead to a substantial loss of time, effort, and resources (Bhojwani and Razdan, 1996; Leifert and Woodward, 1998). Mold contamination in plant tissue cultures is a significant concern that can result in considerable losses (Bhojwani and Razdan, 1996; Leifert and Woodward, 1998). Several strategies can be employed to mitigate contamination. These include using plant genotypes with higher resistance to mold infection and implementing stricter hygiene protocols in laboratory settings (Murashige and Skoog, 1962). Using resistant plant genotypes reduces susceptibility to mold, while rigorous hygiene protocols, including regular sterilization of equipment and workspaces, can minimize the introduction and spread of contaminants (Cassells, 2012). Unfortunately, in cases of contamination, researchers often have no choice but to repeat experiments to salvage their research (Bhojwani and Razdan, 1996; Leifert and Woodward, 1998). To further enhance the sterility of plant tissue cultures, advanced sterilization techniques such as ozone treatment and gamma irradiation can be employed (Murashige and Skoog, 1962). Ozone is a powerful oxidizing agent that can effectively eliminate a wide range of pathogens (Schenk *et al*., 2012), while gamma irradiation penetrates deeply, ensuring thorough sterilization (Leifert and Wooward, 1998). The feasibility of these techniques depends on laboratory settings; for instance, gamma irradiation requires specialized equipment and safety measures, making it suitable for well-equipped labs (Leifert and Wooward, 1998).

Biological contamination is the most important cause of losses in the culture medium. Molds, among the microorganisms, are the most crucial cause of biological contamination in tissue culture studies. Microorganisms that can enter the intercellular spaces of plant tissues can rapidly multiply in the tissues of the explant, obtaining more nutrition sources from the leakage of damaged tissues. Thus, a form of enrichment occurs and can accelerate the death of explants (Leifert and Cassells, 2001). Molds are heterotrophic, eukaryotic microorganisms. They are resistant to harsh environments due to the chitin-rigid cell wall in both hyphae and spores, which protects them from hydrostatic pressure and dryness, as well as pigments such as melanin, which protects them from photooxidation. Being heterotrophs, their ability to secrete various enzymes gives them an advantage in benefiting from all kinds of nutrients in nature and also culture conditions.

As a result of the rapid development of hyphae by spreading by creating anastomosis in the nutrient environment, they completely cover the surface of the environments.

Mold spores and hyphae are ubiquitous in the air and spread in a variety of habitats including terrestrial, aquatic, and atmospheric conditions (Horner, 2003). The numbers and composition of mold in nature can be affected by meteorological conditions, geographical location, vegetation, and human activities such as agriculture. Each geographical region or vegetation has a specialized microhabitat depending on the nutrients. It contains, temperature, water content, and relationships with other microorganisms in that environment. This microhabitat can be infected with guest microorganisms from different environments due to the effects of wind, air pressure, rain drops or the use of agricultural machines/tools used in other soils, and can adapt to that environment and continue their development (Horner, 2003).

Aspergillus and *Penicillium* spp. are the most common molds found in outdoor and indoor environments (Kadaifçiler, 2017; Kadaifciler and Demirel, 2018). Most of them produce phytotoxins, which result in culture mortality, tissue necrosis, and reduces shoot proliferation and rooting (Khan *et al*., 2004). However, mold growth in the nutrient medium can be observed later in culture. *Aspergillus, Penicillium, Alternaria,* and *Fusarium* sp. have been reported to be the major mold contaminants frequently occurring in plant tissue culture (Leifert and Cassells, 2001; Msogoya *et al*., 2012). *Aspergillus* is one of the most abundant and extensively dispersed molds on nature because they evolved a plethora of metabolites to adapt to the various habitats they occupy. That is why they are a key cause of agricultural product degradation. Consequently, they are most often found in terrestrial habitats and are frequently isolated from soil and associated plant litter (Klich, 2002; Samson *et al*., 2010). Some *Aspergillus* species, such as *Aspergillus versicolor,* have been associated with a number of plant diseases despite their saprophytic features (Machida and Gomi, 2010) *Penicillium* species have been isolated from soil and plants, but many are also connected with food spoilage and indoor environments (Samson *et al*., 2010). Similar to *Penicillium*, *Nigrospora* spp. have been isolated from various plant leaves or as saprobes from leaf litter. *Nigrospora* is an important genus with a global distribution and diverse host range (Wang *et al*., 2017). The identification of organisms through culture methods involves allowing them to multiply under specific conditions. This traditional approach, such as quantitative PCR, while effective, is time-consuming and requires specific laboratory conditions and advanced equipment. These constraints often result in inadequate details and procedural limitations. Identification with conventional staining techniques is still widely used in the characterization of microorganisms as a faster, more efficient, and cost-effective alternative.

One of the key effects of mold in plants is the increased production of reactive oxygen species (ROS), leading to an oxidative burst. This burst is the initial step in regulating the plant's systemic acquired resistance (SAR). Excessive ROS production damages critical cellular components, including DNA, proteins, chlorophyll, and cell membranes. If plants are unable to manage this oxidative stress, it can ultimately trigger processes leading to cell death. Antioxidant metabolism, comprising both enzymatic and non-enzymatic agents, plays a crucial role in neutralizing ROS generated under stress conditions. Stress tolerance is closely linked to the activity of antioxidant enzymes, such as catalase (CAT: EC 1.11.1.6), superoxide dismutase (SOD: EC 1.15.1.1), and guaiacol peroxidase (POX: EC 1.11.1.7), as well as the accumulation of non-enzymatic antioxidant compounds (Najafi *et al*., 2024). Proline, an essential osmolyte, helps regulate osmotic pressure and maintain cell integrity. It has been reported to play a significant role in preserving cell structure during fungal pathogen infections, in conjunction with intracellular soluble sugars (Singla *et al*., 2020a; Singla *et al*., 2024).

Raman Spectroscopy (RS) is one of the vibrational spectroscopic methods, and it is a high-output method that allows *in situ* analysis in a short time with less cost, less labour, continuous monitoring of metabolic changes without damaging the plant and ability to provide real-time data (Kuhar *et al*., 2021; Payne and Kurouski, 2021; Saletnik *et al*., 2022). This spectroscopy technique acquires the fingerprint signatures from samples by collecting the inelastically scattered photons as a result of molecular vibrational transitions. These transitions give intrinsic information about the molecular structure of the sample. In our case,

differences of the metabolites produced by the biological samples can be observed in the spectra depending on the environment they are in. Unlike conventional culturing methods, which are time-consuming and often fail to detect non-culturable microbes, Raman spectroscopy provides rapid and comprehensive metabolic profiles. This capability makes it a valuable complement to traditional methods, offering a more holistic view of plant-microbe dynamics and metabolic changes. RS is a method that has been shown to be effective in basic biological research (Gierlinger and Schwanninger, 2007; Schulz and Baranska, 2007), determining the physiological state of plants (Saletnik *et al.*, 2022), product quality, plant species or varieties (Piot *et al.*, 2002; Nikbakht *et al.*, 2011), evaluating the maturity of plants, and pre-symptomatic detection of biotic and abiotic stresses (Skoczowski and Troc, 2013; Altangerel *et al.*, 2017). Raman spectroscopy also facilitates the phenotyping of plants in breeding and the digital selection of new genotypes (Saletnik *et al.*, 2022; Sen *et al.*, 2023).

The aim of this study was to investigate the intricate dynamics of plant-mold interactions in *in vitro* wheat cultures subjected to random mold contaminations, using Raman Spectroscopy (RS) and various biochemical parameters, including chlorophyll, TBARS, proline content, and the activities of antioxidant enzymes (SOD, POX, and CAT), for detailed analysis. It also contributes to the demonstration of the applicability of Raman spectroscopy in basic scientific and agricultural research, and plant breeding programs.

Materials and Methods

Plant material and culture conditions

'Selimiye' wheat cultivar was obtained from Thrace Agricultural Research Institute in Edirne, Türkiye. The outline of the experimental procedure of this study is given in Figure 1. Medium was prepared by the mineral salts of Murashige and Skoog (1962), 0.1 mg/l 2,4-D, 20 g/l sucrose, and 0.8% (w/v) agar. The pH of the media was adjusted to 5.8. The surface sterilization of wheat seeds was done by keeping them in 70% ethanol for 5 min, followed by 5% hypochlorite solution for 20 min, and then rinsing three times with distilled water. The seeds were then imbibed in sterile water for 2h at 35 °C. Mature embryos were removed from the imbibed seeds with the help of a sterile lancet and forceps under aseptic conditions. The mature embryo explants were placed in culture dishes containing the medium. These cultures were then incubated in a growth chamber under a 16h photoperiod, irradiance of 500 μmol m^{-2} s^{-1} photon flux density, and a temperature of 26 °C (Figure 2a) (Kecoglu *et al.*, 2022).

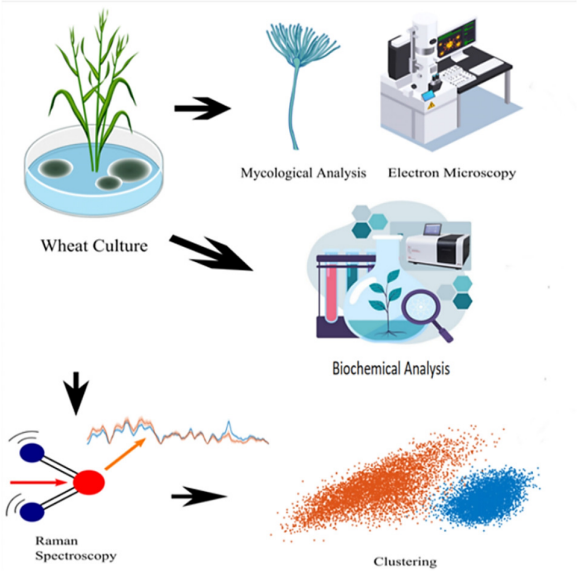

Figure 1. Outline of the experimental procedure

Mycological analyses

Samples were taken by a loop from the parts with mold suspected colonies in different the wheat tissue culture petri dishes (Figure 2b-c), and inoculation was performed into petri plates containing potato dextrose agar (PDA). Sampling and inoculation procedures were performed in duplicate in a sterile cabinet. PDA plates were incubated at 25 °C for 7 days (Belkacem-Hanfi *et al*., 2013). After incubation, growing colonies were examined for their macroscopic and microscopic properties, and then the pure mold colonies were sub-cultured on PDA slants. Mold isolates were inoculated into various media (Czapek yeast autolysate agar, Czapek-Dox agar, Czapek yeast autolysate agar with 20% sucrose, 25% glycerol nitrate agar, malt extract agar) and the plates were incubation at 5 °C, 25 °C, and 37 °C for 7-14 days. After incubation, the isolates taken on the slides were stained with lactophenol cotton blue and examined under a light microscope. They were identified to genus or species level according to their microscopic and colonial characteristics using the identification keys of published guidelines (Barnett, 1955; Ellis, 1971; Pitt, 2000; Klich, 2002).

Scanning Electron Microscope (SEM) analysis

All samples to be surface imaged by SEM for morphological analysis were first coated with a thin layer of gold-palladium at 10 mA for 90 seconds in a vacuum environment of about 1 Pa. To minimize electron beam charging during the SEM measurement, improve sample conductivity, and lessen reflections on the sample surfaces, the pre-measurement process was performed in a vacuum environment utilizing a Quorum-SC7620 device. The Zeiss EVO LS 10 instrument was used to acquire surface morphology images of the samples following the coating procedure. The presence and evolution of contamination on the surfaces of wheat tissue culture samples using SEM imaging was tracked at scale bar of 10 μm. Upon examination of the SEM analysis results, we encountered contamination and subsequent mold in wheat tissue culture structures.

Biochemical analysis

Measurement of total chlorophyll, proline, and lipid peroxidation end products

Leaf tissues were used for the biochemical analyses. Total chlorophyll and carotenoid contents were measured using spectrophotometry, following the method of Lichtenthaler and Wellburn (1983). Proline content was determined using the ninhydrin method (Bates *et al*., 1973). Lipid peroxidation end products were quantified by measuring the amount of thiobarbituric acid-reactive substances (TBARS) through the thiobarbituric acid (TBA) reaction, as described by Heath and Packer (1968).

Measurement of the enzyme activities

200 mg of frozen leaf tissue was extracted using an extraction buffer containing 100 mM phosphate buffer (pH 7.0), 1% polyvinylpyrrolidone 40 (PVP40) (w/v), and 0.1 mM disodium ethylenediaminetetraacetate dihydrate (Na_2-EDTA) to measure the activities of antioxidant enzymes. Homogenates were centrifuged at 13.000 ×g for 25 minutes at 4 °C and the supernatants were used for further analysis. Protein content was measured according to Bradford (Bradford, 1976). Superoxide dismutase (SOD, EC:1.15.1.1) activity was assayed by monitoring the superoxide radical-induced nitro blue tetrazolium chloride (NBT) reduction at 560 nm (Beauchamp and Fridovich, 1971). One unit of SOD activity was characterized as the amount of enzyme, which leads to a 50% inhibition of the photochemical reduction of NBT. The measurement of peroxidase (POX, EC:1.11.1.7) activity was measured at 470 nm by using, and guaiacol as substrates. The disappearance of H_2O_2 was monitored at 240 nm for the determination of catalase (CAT, EC:1.11.1.6) activity (Aebi, 1984).

Raman spectroscopy setup

We utilized a custom-built Raman spectroscopy setup for the measurements. This setup uses a 500 mW 785 nm diode laser as the excitation source whose power output in the back-focal is 50 mW after the beam shape correction and the losses from the optics. We steer the beam into the microscope objective (0.4 NA, 20x,

Plan-Neofluar, Carl Zeiss Microscopy) using consecutive silver and dichroic mirrors (Thorlabs). The same microscope objective also collects the Raman scattered photons, and they travel the same path in the opposite direction until they reach the dichroic mirror (DMLP 805, Thorlabs), where they are separated from the rest of the optical path. Thereafter, the Raman signal gets cleaned using two consecutive Raman edge filters and then coupled into a 0.22 NA multimode fibre connected to the Raman spectrometer (QE-Pro, Ocean Insight). Above the objective, we have a sample holder attached to a motorized XY stage (8MTF-102LS05, Standa), using which we have scanned the leaf samples (Klich, 2002; Sen *et al*., 2023).

Data collection

We have measured two different classes of samples. The first was from a plant sample with visible mold development. The second was the control sample for the first one, without mold growth. From two groups, we have taken two samples of leaves and scanned a region of 10 mm by 1 mm with 50 mm step size on them. We collected 4221 spectra from different points on the leaf sample with each scan. Since we examined two separate leaves from each group, we had 8442 spectra in total for each group (Kecoglu *et al*., 2022; Sen *et al*., 2023).

Data analysis

To quantify the biochemical parameters, leaves were randomly pooled from three seedlings in each group. Statistical analysis was performed using one-way analysis of variance (ANOVA) on the spectrophotometric data. The Shapiro-Wilk test was employed to assess the normality of the data, and differences between exposure groups were further analyzed using ANOVA followed by Tukey's post-hoc test. A p-value of less than 0.05 was considered statistically significant (Zar, 1984).

We eliminated outliers from the Raman spectral dataset by removing the spectra outside the 0.3%-99.7% quartile range. We then balanced class sizes by reducing larger classes to the smallest class size through random sampling. The mean of these spectra with their standard deviation is given in Figure 5a. Next, we performed Principal Component Analysis (PCA) for dimensional reduction. To better visualize the separation between the classes, we have scattered the data into the space of the first two principal components (PC). We randomly split the dataset into 80%-20% train-test sets while preserving the class balance for model training and testing. Then, we trained a Linear Discriminant Analysis (LDA) model using the training set (80% of the data) and tested it on the test set (remaining 20%), resulting in the confusion matrix shown in Figure 5d. To better visualize the chemical difference between the classes, we produced the violin plots of the normalized Raman intensities of groups against each other for 747, 913, and 1519 cm^{-1}, given in Figure 6. All the analysis was conducted using MATLAB (R2022b, The MathWorksInc.). The violin plots were produced using the publicly available function violin at MathWorks File Exchange (Hoffmann, 2015).

Results

Mold identification

The presence of *Aspergillus versicolor* (Vuill.) Tirab., 1908 and *Penicillium* sp. Link, 1809 was established in wheat tissue cultures (Figure 2b-c) using traditional culture techniques. Light Microscopy (LM) imaging confirmed these findings, showcasing the main structure of *Aspergillus versicolor* in Figure 3a, characterized by an unbranched stipe and a radiate-shaped conidial head. This suggests that it can survive on dried grains at lower temperatures (Samson *et al*., 2010). *Penicillium* sp., depicted in Figure 3b, exhibits conidia chains produced by phialides, making it a frequent contaminant on various substrates (Samson *et al*., 2010). Additionally, *Nigrospora* sp. Zimm., 1902, was identified, characterized by solitary black conidia and micronematous, branching conidiophores, as shown in Figure 3c. *Nigrospora* species, commonly found in

tropical regions, have been reported to be plant pathogens in economically important crops and ornamental plants (Ellis, 1971).

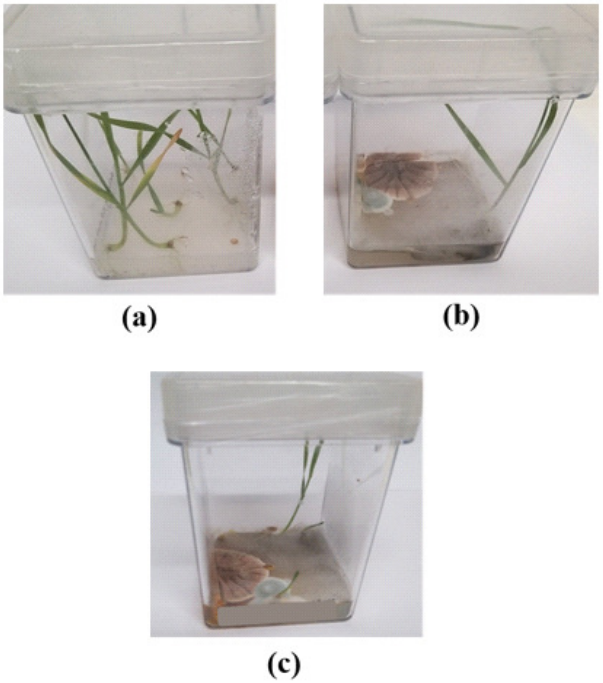

Figure 2. Examples of tissue culture container in which seeds are planted and growth occurs: a) Uncontaminated pattern, b-c) Contaminated pattern covered by mold suspected colonies

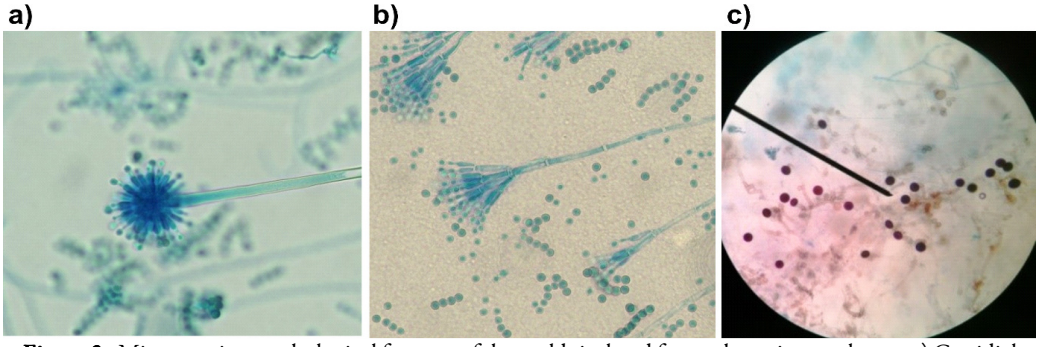

Figure 3. Microscopic morphological features of the molds isolated from wheat tissue cultures: a) Conidial head, spores and unbranched stipe of *Aspergillus versicolor*. b) Typical Penicilli structure including conidia, phialides, metulae and stipe of *Penicillium* sp. c) Conidiogenous cells giving rise to conidia of *Nigrospora* sp. (magnification × 400)

SEM imaging

The progression and presence of contamination on wheat tissue culture samples were monitored through Scanning Electron Microscopy (SEM), with detailed scale bars of 10 µm presented in Figure 4a–f. The images clearly illustrated mold structures on the surface of the wheat tissue culture, indicating a homogeneous distribution of mold hyphae across the plant surface, in contrast to the more localized positioning of spores (Figure 4c-f).

Integrating real-time SEM imaging with artificial intelligence (AI) can revolutionize mold monitoring and intervention. AI algorithms can analyze SEM images to detect early signs of mold growth, providing alerts for immediate action. This integration enables continuous, automated monitoring of cultures, enhancing early detection and allowing timely interventions to prevent widespread contamination.

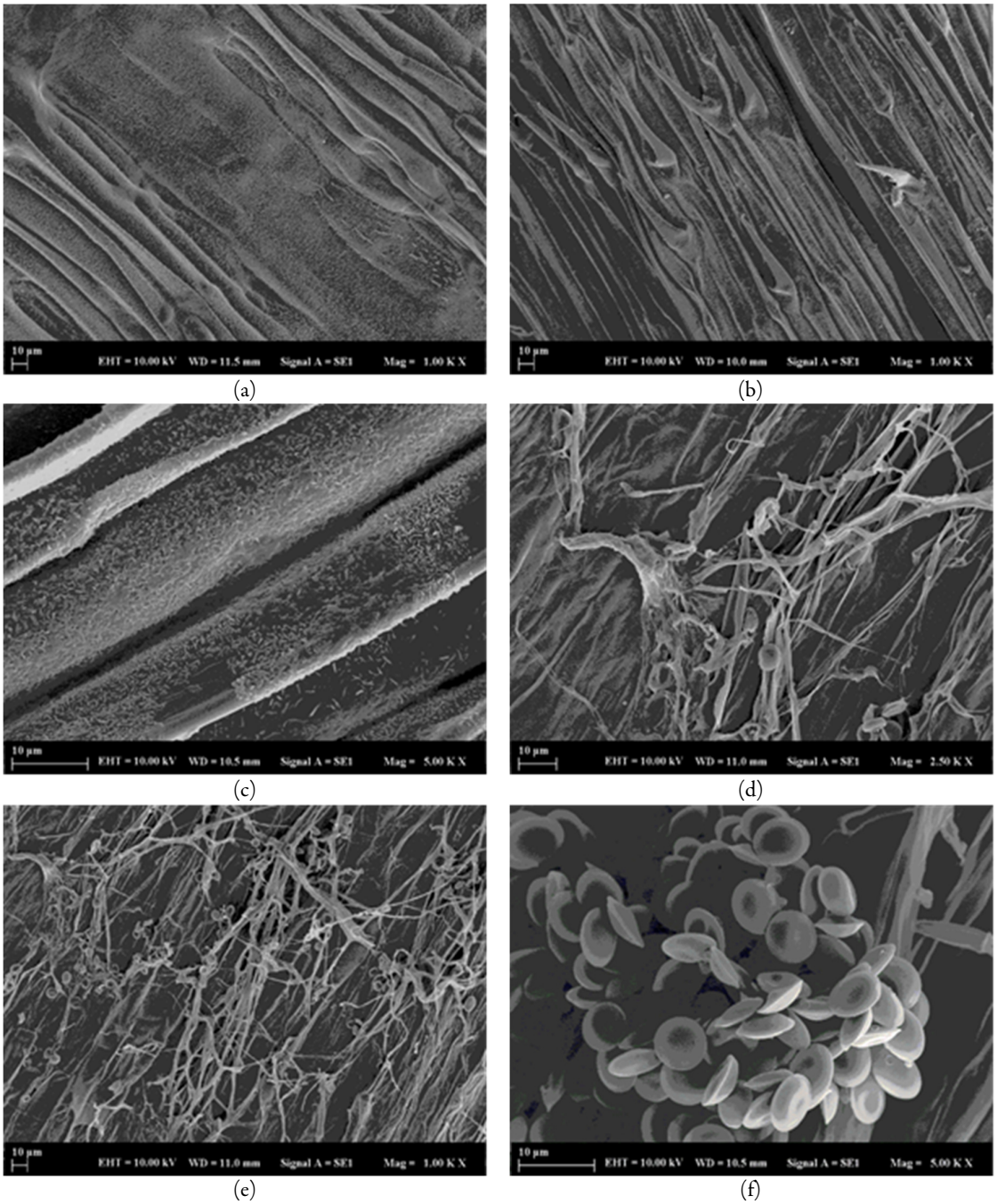

Figure 4. Monitoring the contamination's evolution with SEM imaging on wheat tissue culture samples' surfaces: a-b) Uncontaminated patterns, c-d) Patterns where surface mold contamination has started to form, e-f) Patterns where the surface contamination is completely covered and mold hyphae and spores are present

Biochemical analysis

A statistically significant decrease was observed in the chlorophyll (61.92%, ***$p < 0.001$) and carotenoid (65.94%, ***$p < 0.001$) contents, alongside a significant increase in TBARS levels (150.02%, ***$p < 0.001$), all of which are indicators of cell damage under stress, in the experimental group exposed to mold contamination compared to the control group (Table 1).

While the increase in proline content (21.98%, ns), an intracellular defense marker, was not statistically significant compared to the control, the activities of antioxidant enzymes SOD (59.69%, **$p < 0.01$), POX (42.09%, **$p < 0.01$), and CAT (63.59%, **$p < 0.01$) showed statistically significant increases in response to mold contamination (Table 1).

Table 1. Changes in biochemical parameters in control and mold-contaminated experimental groups

Biochemical Parameters	Control	Mold-contaminated
Chlorophyll ($mg(gFW)^{-1}$)	1.187±0.232	0.452±0.034***
Carotenoids ($mg(gFW)^{-1}$)	0.875±0.095	0.298±0.023***
TBARS ($nmol(gFW)^{-1}$)	2.305±0.347	5.763±0.645***
Proline($\mu mol(mgprotein)^{-1}$)	2.653±0.433	3.236±0.452^{ns}
SOD ($U(mgprotein)^{-1}$)	20.342±2.976	32.485±8.228**
POX ($\Delta A_{470}(mgprotein)^{-1}$)	35.436±5.348	50.326±9.547**
CAT ($U(mgprotein)^{-1}$)	1.807±0.093	2.956±0.198**

Significant differences were determined according to Tukey's HSD test at **$p < 0.01$, ***$p < 0.001$, ns: not significant.
The values are means and standard errors for five replications of the experimental groups.

Raman spectroscopy analysis

A comparative analysis of the average normalized Raman spectra between mold-infected and non-infected samples was conducted (Figure 5a), revealing significant differences in normalized intensities across various Raman bands. Some particular Raman shift values whose corresponding assignments can be seen in Table 2 were marked. Specifically, normalized intensities at 814, 940, 1066, 1110, 1519, 1543, and 1606 cm^{-1} exhibited considerable variation, while bands at 445, 611, 724, 864, 995, 1324, and 1489 cm^{-1} were similar, and bands at 509, 747, 913, 1153, 1186, 1222, 1247, 1282 cm^{-1} showed negligible change. The most substantial change was noted at 1519 cm^{-1}, generally associated with carotenoids, indicating a decrease in level between control and mold infected plants (Jehlička *et al*., 2014; Morey *et al*., 2021). From Figure 5b, it is apparent that the first two PCs were enough to separate control and mold infected plant data. Consequently, we used only these two components to classify the data. After the PCA, we also plotted the loadings (Figure 5c), which indicates which Raman bands are more responsible for the deviation between the classes.

Discriminant analysis and biochemical characterization

Utilizing Linear Discriminant Analysis (LDA) and generating violin plots for specific Raman bands, we further characterized the biochemical impacts of mold contamination. The model's performance, represented by the confusion matrix in Figure 5d, demonstrated high accuracy, precision, and sensitivity, with metrics approximately at 0.988, 0.977, and 0.999, respectively, and an F1-score of about 0.988. This emphasizes the potential of handheld Raman systems for non-destructive field assessments of plant health. The confusion matrix results highlight the model's accuracy, precision, and areas for improvement in real-time monitoring systems. By analysing the matrix, researchers can identify specific classes where misclassifications occur, informing targeted refinements in the model. These refinements could include enhancing the training dataset, improving feature selection, or integrating additional data sources to increase overall accuracy and precision. Figure 6 shows comparative differences in biochemical responses between plant parts affected and unaffected by mold contamination.

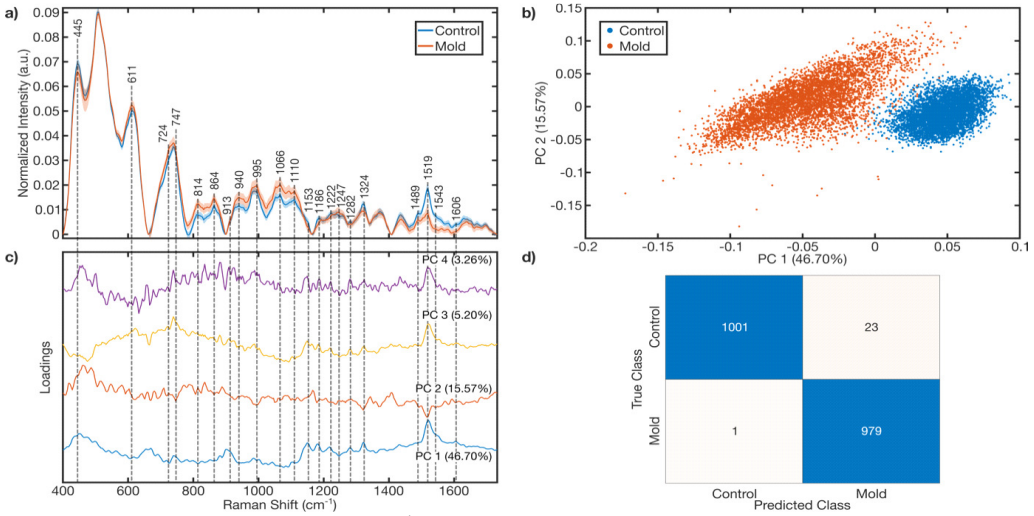

Figure 5. Raman spectroscopy results. a) Mean spectra with the standard deviation as a shaded graph. Dashed lines mark some important Raman shift values discussed in the text. b) The scattering of the data on PC 1 – PC 2 space. The total variance explained by each principal component is given in the parenthesis at each axis. c) The PCA loading plot, which indicates the most significant bands creating the separation between the groups. d) The confusion matrix of the trained LDA model used on the test set

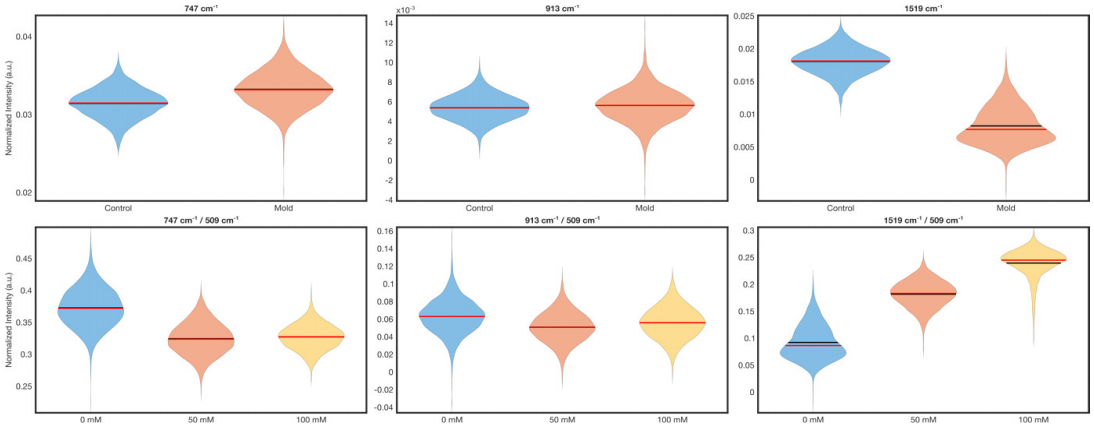

Figure 6. Violin plots. The top row compares the distributions of mold samples against the control samples. The bottom row compares the different mold samples against each other. The red lines indicate the median, and the black lines indicate the mean of the distributions

Discussion

This study focuses on investigating the intricate dynamics of plant-mold interactions in *in vitro* conditions, employing a multi-method approach to investigate incidental contaminations in wheat tissue cultures. This approach began with identification through conventional culture techniques, followed by visualization of the contaminants using Light Microscopy (LM) and Scanning Electron Microscopy (SEM) imaging, and characterization of biochemical differentiation induced by these contaminations using biochemical parameters (such as chlorophyll, TBARS, proline content, and the activities of antioxidant enzymes (SOD, POX, and CAT)) and Raman Spectroscopy.

Table 2. Tentative band assignments for the changing peak wave numbers

Peak (cm^{-1})	Change (from control to mold, shift and/or intensity)	Assignment	Reference
445	Decrease	Si-O-Si Stretching	(HORIBA Scientific, 2024)
509	Decrease	S-S bond stretching (disulfide bridges in proteins)	(*HORIBA Scientific*, 2024)
611	Decrease	Ti-O Bond Stretching	(*HORIBA Scientific*, 2024)
724	Increase	C-C stretching (aliphatic chains)	(Morey *et al*., 2021)
747	Increase	Pyranose ring stretching	(Synytsya *et al*., 2003)
814	Increase	C-H bending (polysaccharides)	(Synytsya *et al*., 2003)
864	Increase	γ(CH)from carbohydrates	(Espina *et al*., 2022)
913	Decrease	C-O-C ring deformation	(Zhu *et al*., 2011)
940	Increase	Skeletal C-C stretch	(Zhu *et al*., 2011
995	Decrease	AromaticC-H stretching	(Zhu *et al*., 2011
1066	Increase	C-H bending (proteins)	(Zhu *et al*., 2011
1100	Decrease	C-O stretching	(Synytsya *et al*., 2003)
1153	Increase	Skeletal C-O and C-C vibration	(Synytsya *et al*., 2003)
1186	Increase	CH deformation	(Synytsya *et al*., 2003)
1222	Increase	C-Cstretching (glycosides)	(Synytsya *et al*., 2003)
1247	Decrease	C-OH bending	(Zhu *et al*., 2011)
1282	Increase	C-C stretching in lipids	(Zhu *et al*., 2011)
1324	Increase	Aromatic C-H bending	(Zhu *et al*., 2011)
1489	Decrease	C-H bending (lipids)	(Schulz and Baranska, 2007)
1519	Decrease	v(C=C), β-carotene	(Jehlička *et al*., 2014a; Jehlička *et al*., 2014b)
1543	Decrease	Amide II, proteins	(HORIBA Scientific, 2024)
1606	Decrease	C=C stretching (aromatic compounds)	(Morey *et al*., 2021)

Interdisciplinary research combining plant pathology and environmental monitoring is crucial for understanding and managing mold growth in agricultural systems. Collaborative efforts can develop comprehensive monitoring strategies that account for environmental factors influencing mold growth. For instance, combining data from weather monitoring systems with plant health diagnostics can provide insights into conditions that favour mold proliferation, thereby informing better management practices (Kuska *et al*., 2022).

The detection of *Aspergillus versicolor* and *Penicillium* sp. in wheat tissue cultures underscores the pervasive risk of mold contamination from soil and airborne spores. Also, the findings highlight the challenge posed by the presence of mold spores and hyphae in both indoor and outdoor environments in maintaining sterile conditions in tissue cultures. SEM imaging provided information about the distribution of contaminants on the plant, while supporting light microscopy provided detailed information about their structural properties. The structural characteristics of these molds, as depicted in Figure 3a for *Aspergillus versicolor* and Figure 3b for *Penicillium* sp., provide insights into their adaptability and survival mechanisms in various environments, both indoors and outdoors. The resilience of these species to temperature and humidity variations highlights the necessity for vigilant monitoring and management practices in agricultural and indoor settings (Klich, 2002; Samson *et al*., 2010).

SEM images (Figures 4a–f) reveal extensive mold colonization on plant surfaces, indicating a homogeneous distribution pattern of mold hyphae and spores. This distribution suggests strategic adaptations by molds to maximize nutrient acquisition and reproductive success on host plant surfaces. Molds like *Aspergillus* and *Penicillium* secrete enzymes that degrade plant cell walls, releasing nutrients (Klich, 2002; Samson *et al*., 2010). Each mold species identified more pronounced induces specific biochemical alterations in plant metabolism than others. For instance, *Aspergillus versicolor* reduces carotenoid levels, affecting photosynthesis and overall plant health, while *Penicillium* sp. alters chlorophyll content, impacting photosynthetic efficiency. *Nigrospora* sp. produces enzymes that degrade cell walls, leading to nutrient leakage and tissue damage. Understanding these specific impacts helps in developing targeted strategies for mitigating mold-induced damage.

One of the initial steps in plant-pathogen interaction is the activation of systemic acquired immunity (SAI), which triggers an oxidative burst during pathogenesis. This oxidative burst occurs in two phases: an initial, short-lived burst immediately after the pathogen attack, followed by a longer-lasting burst that occurs hours after contamination. The reactive oxygen species (ROS) generated during these bursts serve two key functions: they activate the plant's intracellular defense system and act as secondary signalling molecules. In addition to their role in signalling, ROS, such as superoxide radicals, hydrogen peroxide, and hydroxyl radicals, trigger the activation of the plant's antioxidant defense system, which includes both enzymatic and non-enzymatic components that help maintain cellular balance. Superoxide dismutase (SOD), one of the primary antioxidant enzymes, converts superoxide radicals into hydrogen peroxide, which is then neutralized by catalase (CAT) and peroxidase (POX) enzymes (Singla *et al*., 2020; Najafi *et al*., 2024). Najafi *et al*. (2024) reported that *P. melonis* enhanced the expression of enzymes such as POX, SOD, CAT, PPO, PAL, glucanase, and increased phenolic content in a resistant cultivar against pumpkin blight infection. Similarly, Singla *et al*. 2024 observed elevated activities of antioxidant enzymes, including SOD, CAT, POX, NADPH oxidase, APX, and GST, in barley during strip rust infection, findings that are consistent with our study. In another study on strip rust in barley, (Singla *et al*., 2020b) also reported an increase in proline, a key intracellular osmolyte. Although proline levels increased in our study, the change was not statistically significant. Proline is recognized in the literature as an essential osmolyte involved in various intracellular processes, ranging from maintaining cell integrity to supporting cell division under both biotic and abiotic stress conditions (Singla *et al*., 2020a; Sen *et al*., 2023). Despite the activation of intracellular defense mechanisms in our study, the observed decrease in chlorophyll and carotenoid levels, both indicators of stress-related cell damage, and the significant increase in TBARS (a marker of lipid peroxidation in cell membranes), suggest that these defense responses were insufficient to fully mitigate cell damage during pathogenesis.

Raman spectroscopy provided a detailed biochemical perspective on mold contamination impacts. It revealed significant changes in Raman spectra between mold-infected and uninfected plant samples, particularly in regions associated with vital photosynthetic pigments such as carotenoids and chlorophyll. The significant spectral differences observed between mold-infected and non-infected samples, particularly at bands associated with carotenoids (1519 cm^{-1}) and chlorophyll (1282, 1324 and 1606 cm^{-1}), reflect profound biochemical alterations induced by mold infection presence. These alterations suggest a detrimental impact of mold contamination on plant health, particularly through reduced photosynthetic efficiency, as evidenced by the decrease in carotenoid and chlorophyll levels. As a matter of fact, it has been reported that the decrease in carotenoid and chlorophyll levels in infected samples can have significant effects on plant health, affecting photosynthetic efficiency and overall viability (Jehlička *et al*., 2014a; Jehlička *et al*., 2014b; Tatagiba *et al*., 2015; Egging *et al*., 2018; Morey *et al*., 2021). The underlying reason for this is that mold infection causes leaf surfaces to be covered with spores and hyphae, which limits the amount of light reaching the underlying cells. This disruption in light exposure interferes with metabolic reactions and leads to an increase in reactive oxygen species (ROS) within the cells. The observed increase in the Raman bands attributed to carbohydrates (814,

864, and 1222 cm^{-1}) indicates that carbohydrate-derived intracellular osmolytes, along with proline, play a significant role in maintaining cell integrity and vitality.

The application of Linear Discriminant Analysis (LDA), as demonstrated by the performance metrics and confusion matrix in Figure 5d, illustrates the potential of Raman spectroscopy in accurately distinguishing between mold-infected and non-infected plant samples. These results, showing high accuracy, precision, and sensitivity, highlight the feasibility of handheld Raman systems for in-field diagnostics. The study's violin plots further elucidated the biochemical impacts of mold contamination, providing a nuanced comparison between affected and unaffected plant tissues. Notably, in Figure 6, the consistent levels of glycine across samples indicate that certain metabolic processes may remain unaffected by mold presence, offering a glimmer of resilience amid the detrimental effects of contamination. Indeed, it has been reported in previous publications that glycine plays an important role in the oxidative stress response caused by biotic stress factors to eliminate the harmful effects of ROS and to maintain intracellular metabolic integrity (Czolpinska and Rurek, 2018).

Conclusions

To conclude, this study has demonstrated the utility of advanced analytical techniques such as SEM and Raman spectroscopy in addition to conventional biochemical analyses to reveal the harmful effects of random mold contamination in plant tissue culture medium on plant physiological processes. It also provides contributions to the international literature on optimizing Raman spectroscopy methodologies for real-time monitoring and the integration of these techniques into basic scientific research, agricultural practices and plant breeding programs. The fact that high-throughput data obtained with Raman spectroscopy contribute to new analyses in different research areas such as artificial intelligence, machine learning and deep learning, which have become increasingly popular in recent years, deepens the dimension of our study.

Authors' Contributions

Conceptualization: AS; Study design and methodology: AS, F.G. and D.G.-K.; Data collection, A.S., O.D., M.A., F.G., and D.G.-K. Analysis A.S., F.G., D.G.-K.; Writing, A.S., F.G., D.G.-K.; Supervision, A.S. to M.A., and O.D. All authors read and approved the final manuscript.

Ethical approval (for researches involving animals or humans)

Not applicable.

Funding

This study was supported by The Research Fund of Istanbul University by Project Numbers: 32759, 49463 and FDK-2024-41013 to AS.

Acknowledgements

All authors would like to thank Prof. Dr. Mehmet Burcin Unlu, Dr. Ugur Parlatan and BSc. Ibrahim Kecoglu for opening their laboratories in the Physics Department of Boğaziçi University, (İstanbul, Türkiye)

and supporting us in Raman Spectroscopy analysis. All authors have read and agreed to the published version of the manuscript.

Conflict of Interests

The authors declare that there are no conflicts of interest related to this article.

References

Aebi H (1984). Catalase *in vitro*. In: Methods in Enzymology. Academic press, pp 121-126. *https://doi.org/10.1016/S0076-6879(84)05016-3*

Altangerel N, Ariunbold GO, Gorman C, Alkahtani MH, Borrego EJ, Bohlmeyer D, ... Scully MO (2017). *In vivo* diagnostics of early abiotic plant stress response via Raman spectroscopy. Proceedings of the National Academy of Sciences 114(13):3393-3396. *https://doi.org/10.1073/pnas.1701328114*

Barnett HL (1955). Illustrated genera of imperfect fungi. *https://www.cabidigitallibrary.org/doi/full/10.5555/19561100378*

Bates LS, Waldren RPA, Teare ID (1973). Rapid determination of free proline for water-stress studies. Plant and Soil 39:205-207. *https://doi.org/10.1007/BF00018060*

Beauchamp C, Fridovich I (1971). Superoxide dismutase: improved assays and an assay applicable to acrylamide gels. Analytical Biochemistry 44(1):276-287. *https://doi.org/10.1016/0003-2697(71)90370-8*

Beck JJ, Alborn HT, Block AK, Christensen SA, Hunter CT, Rering CC, ... Tumlinson JH (2018). Interactions among plants, insects, and microbes: elucidation of inter-organismal chemical communications in agricultural ecology. Journal of Agricultural and Food Chemistry 66(26):6663-6674. *https://doi.org/10.1021/acs.jafc.8b01763*

Belkacem-Hanfi N, Semmar N, Perraud-Gaime I, Guesmi A, Cherni M, Cherif I, ... Roussos S (2013). Spatio-temporal analysis of post-harvest moulds genera distribution on stored durum wheat cultivated in Tunisia. Journal of Stored Products Research 55:116-123. *https://doi.org/10.1016/j.jspr.2013.08.008*

Bever JD, Westover KM, Antonovics J (1997). Incorporating the soil community into plant population dynamics: the utility of the feedback approach. Journal of Ecology 561-573. *https://doi.org/10.2307/2960528*

Bhojwani SS, Razdan MK (1996). Plant tissue culture: theory and practice. Elsevier.eBook ISBN: 9780080539096.

Bradford MM (1976). A rapid and sensitive method for the quantitation of microgram quantities of protein utilizing the principle of protein-dye binding. Analytical Biochemistry 72(1-2):248-254. *https://doi.org/10.1016/0003-2697(76)90527-3*

Cassells AC (2012). Pathogen and biological contamination management in plant tissue culture: phytopathogens, *vitro* pathogens, and *vitro* pests. Plant Cell Culture Protocols 57-80. *https://doi.org/10.1007/978-1-61779-818-4_6*

Czolpinska M, Rurek M (2018). Plant glycine-rich proteins in stress response: an emerging, still prospective story. Frontiers in Plant Science 9:302. *https://doi.org/10.3389/fpls.2018.00302*

Egging V, Nguyen J, Kurouski D (2018). Detection and identification of fungal infections in intact wheat and sorghum grain using a hand-held Raman spectrometer. Analytical Chemistry 90(14):8616-8621. *https://doi.org/10.1021/acs.analchem.8b01863*

Ellis MB (1971). Dematiaceous hyphomycetes. Commonwealth Mycological Institute, pp 608.

Espina A, Cañamares MV, Jurasekova Z, Sanchez-Cortes S (2022). Analysis of iron complexes of tannic acid and other related polyphenols as revealed by spectroscopic techniques: Implications in the identification and characterization of iron gall inks in historical manuscripts. ACS Omega 7(32):27937-27949. *https://doi.org/10.1021/acsomega.2c01679*

Gierlinger N, Schwanninger M (2007). The potential of Raman microscopy and Raman imaging in plant research. Spectroscopy 21(2):69-89. *https://content.iospress.com/articles/spectroscopy/spe302*

Heath RL, Packer L (1968). Photoperoxidation in isolated chloroplasts: I. Kinetics and stoichiometry of fatty acid peroxidation. Archives of Biochemistry and Biophysics 125(1):189-198. *https://doi.org/10.1016/0003-9861(68)90654-1*

Hoffmann, H. (2015). violin. m-Simple violin plot using matlab default kernel density estimation. INRES (University of Bonn), Katzenburgweg 5:53115.

"HORIBA Scientific." Accessed: Sep. 22, 2024. *https://www.horiba.com/int/scientific/?utm_source=uhw&utm_medium=301&utm_campaign=uhw-redirect*

Horner WE (2003). Assessment of the indoor environment: evaluation of mold growth indoors. Immunology and Allergy Clinics 23(3):519-531. *https://www.immunology.theclinics.com/article/S0889-8561(03)00063-8/abstract#page-body-id*

Hussain A, Qarshi IA, Nazir H, Ullah I (2012). Plant tissue culture: current status and opportunities. Recent Advances in Plant In Vitro Culture 6(10):1-28.

Jehlička J, Edwards HG, Osterrothov K, Novotn J, Nedbalov L, Kopecký J, ... Oren A (2014a). Potential and limits of Raman spectroscopy for carotenoid detection in microorganisms: implications for astrobiology. Philosophical Transactions of the Royal Society A: Mathematical, Physical and Engineering Sciences 372(2030):20140199. *https://doi.org/10.1098/rsta.2014.0199*

Jehlička J, Edwards HG, Oren A (2014b). Raman spectroscopy of microbial pigments. Applied and Environmental Microbiology 80(11):3286-3295. *https://doi.org/10.1128/AEM.00699-14*

Kadaifciler DG, Demirel R (2018). Fungal contaminants in man-made water systems connected to municipal water. Journal of Water and Health 16(2):244-252. *https://doi.org/10.2166/wh.2018.272*

Kadaifçiler DG (2017). Airborne fungi in the atmosphere in Beyazıt Square, Istanbul, Turkey. Celal Bayar University Journal of Science 13(2):343-351. *https://dergipark.org.tr/en/pub/cbayarfbe/issue/29779/319820*

Kecoglu I, Sirkeci M, Unlu MB, Sen A, Parlatan U, Guzelcimen F (2022). Quantification of salt stress in wheat leaves by Raman spectroscopy and machine learning. Scientific Reports 12(1):7197. *https://www.nature.com/articles/s41598-022-10767-y*

Khan IA, Alam SS, Jabbar A (2004). Purification of phytotoxin from culture filtrates of *Fusarium oxysporum* f. sp. *ciceris* and its biological effects on chickpea. Pakistan Journal of Botany 36(4):871-880. *https://www.pakbs.org/pjbot/PDFs/36(4)/PJB36(4)871.pdf*

Klich MA (2002). Identification of common *Aspergillus* species. Centraalbureau voor Schimmelcultures, Utrecht, The Netherlands.

Kuhar N, Sil S, Umapathy S (2021). Potential of Raman spectroscopic techniques to study proteins. Spectrochimica Acta Part A: Molecular and Biomolecular Spectroscopy 258:119712. *https://doi.org/10.1016/j.saa.2021.119712*

Kuska MT, Heim RH, Geedicke I, Gold KM, Brugger A, Paulus S (2022). Digital plant pathology: A foundation and guide to modern agriculture. Journal of Plant Diseases and Protection 129(3):457-468. *https://doi.org/10.1007/s41348-022-00600-z*

Leifert C, Woodward S (1998). Laboratory contamination management: the requirement for microbiological quality assurance. Plant Cell, Tissue and Organ Culture 52:83-88. *https://link.springer.com/chapter/10.1007/978-94-015-8951-2_30*

Leifert C, Cassells AC (2001). Microbial hazards in plant tissue and cell cultures. In Vitro Cellular & Developmental Biology-Plant 37:133-138. *https://link.springer.com/article/10.1007/s11627-001-0025-y*

Lichtenthaler HK, Wellburn AR (1983). Determinations of total carotenoids and chlorophylls a and b of leaf extracts in different solvents. Biochemical Society Transactions 11(5):591-592. *https://doi.org/10.1042/bst0110591*

Machida M, Gomi K (2010). Aspergillus: molecular biology and genomics. Caister Academic Press. *https://doi.org/10.21775/9781910190159*

Morey R, Farber C, McCutchen B, Burow MD, Simpson C, Kurouski D, Cason J (2021). Raman spectroscopy-based diagnostics of water deficit and salinity stresses in two accessions of peanut. Plant Direct 5(8):e342. *https://doi.org/10.1002/pld3.342*

Msogoya TJ, Kanyagha H, Mutigitu J, Kulebelwa M, Mamiro D (2012). Identification and management of microbial contaminants of banana *in vitro* cultures. Journal of Applied Biosciences 55:3987-3994 *https://m.elewa.org/JABS/2012/55/5.pdf*

Murashige T, Skoog F (1962). A revised medium for rapid growth and bio assays with tobacco tissue cultures. Physiologia Plantarum 15(3). *https://doi.org/10.1111/j.1399-3054.1962*

Najafi M, Esfahani MN, Vatandoost J, Hassanzadeh-Khankahdani H, Moeini MJ (2024). Antioxidant enzymes activity associated with resistance to *Phytophthora melonis*-pumpkin blight. Physiological and Molecular Plant Pathology 129:102192. *https://doi.org/10.1016/j.pmpp.2023.102192*

Nikbakht AM, Tavakkoli HT, Malekfar R, Gobadian B (2011). Nondestructive determination of tomato fruit quality parameters using Raman spectroscopy. Journal of Agricultural Science and Technology 13:517-526.

Payne WZ, Kurouski D (2021). Raman spectroscopy enables phenotyping and assessment of nutrition values of plants: a review. Plant Methods 17(1):78. *https://link.springer.com/article/10.1186/s13007-021-00781-y*

Piot O, Autran JC, Manfait M (2002). Assessment of cereal quality by micro-Raman analysis of the grain molecular composition. Applied Spectroscopy 56(9):1132-1138. *https://opg.optica.org/as/abstract.cfm?uri=as-56-9-1132*

Pitt JI (2000). A laboratory guide to common Penicillium species, 3th ed., Food Science Australia, North Ryde NSW, Australia.

Saletnik A, Saletnik B, Puchalski C (2022). Raman method in identification of species and varieties, assessment of plant maturity and crop quality—A review. Molecules 27(14):4454. *https://doi.org/10.3390/molecules27144454*

Samson RA, Houbraken J, Thrane U, Frisvad JC, Andersen B (2010). Food and indoor fungi: CBS-KNAW fungal biodiversity centre. CBS-KNAW Fungal Biodiversity Centre, Utrecht, the Netherlands. *https://doi.org/10.3920/9789086867226_006*

Schenk PM, Carvalhais LC, Kazan K (2012). Unraveling plant–microbe interactions: can multi-species transcriptomics help?. Trends in Biotechnology 30(3):177-184.

Schulz H, Baranska M (2007). Identification and quantification of valuable plant substances by IR and Raman spectroscopy. Vibrational Spectroscopy 43(1):13-25. *https://doi.org/10.1016/j.vibspec.2006.06.001*

Sen A, Kecoglu I, Ahmed M, Parlatan U, Unlu MB (2023). Differentiation of advanced generation mutant wheat lines: Conventional techniques versus Raman spectroscopy. Frontiers in Plant Science 14:1116876. *https://doi.org/10.3389/fpls.2023.1116876*

Singla P, Bhardwaj RD, Kaur S, Kaur J, Grewal SK (2020a). Metabolic adjustments during compatible interaction between barley genotypes and stripe rust pathogen. Plant Physiology and Biochemistry 147:295-302. *https://doi.org/10.1016/j.plaphy.2019.12.030*

Singla P, Bhardwaj RD, Kaur S, Kaur J (2020b). Stripe rust induced defence mechanisms in the leaves of contrasting barley genotypes (*Hordeum vulgare* L.) at the seedling stage. Protoplasma 257:169-181. *https://link.springer.com/article/10.1007/s00709-019-01428-5*

Singla P, Bhardwaj RD, Sunidhi SS (2024). Plant–fungus interaction: a stimulus–response theory. Journal of Plant Growth Regulation 43(2):369-381. *https://link.springer.com/article/10.1007/s00344-023-11100-1*

Skoczowski A, Troć M (2013). Isothermal calorimetry and Raman spectroscopy to study response of plants to abiotic and biotic stresses. Molecular Stress Physiology of Plants 263-288. *https://doi.org/10.1007/978-81-322-0807-5_11*

Smith SE, Read DJ (2010). Mycorrhizal symbiosis. Academic press.

Synytsya A, Čopíková J, Matějka P, Machovič VJCP (2003). Fourier transform Raman and infrared spectroscopy of pectins. Carbohydrate Polymers 54(1):97-106. *https://doi.org/10.1016/S0144-8617(03)00158-9*

Tatagiba SD, DaMatta FM, Rodrigues FÁ (2015). Leaf gas exchange and chlorophyll a fluorescence imaging of rice leaves infected with *Monographella albescens*. Phytopathology 105(2):180-188. *https://doi.org/10.1094/PHYTO-04-14-0097-R*

Wang M, Liu F, Crous PW, Cai L (2017). Phylogenetic reassessment of *Nigrospora*: ubiquitous endophytes, plant and human pathogens. Persoonia-Molecular Phylogeny and Evolution of Fungi 39(1):118-142. *https://doi.org/10.3767/persoonia.2017.39.06*

Whitham TG, Gehring CA, Evans LM, LeRoy CJ, Bangert RK, Schweitzer JA, ... Bailey JK (2010). A community and ecosystem genetics approach to conservation biology and management. Molecular approaches in natural resource conservation and management. Cambridge Univ. Press, Cambridge, UK, pp 50-73.

Zar JH (1984). Biostatistical analysis. Prentice-Hall Inc, Englewood Cliffs, Jersey.

Zhang H, Zhao Y, Zhu JK (2020). Thriving under stress: how plants balance growth and the stress response. Developmental Cell 55(5):529-543. *https://doi.org/10.1016/j.devcel.2020.10.012*

Zhu G, Zhu X, Fan Q, Wan X (2011). Raman spectra of amino acids and their aqueous solutions. Spectrochimica Acta Part A: Molecular and Biomolecular Spectroscopy 78(3):1187-1195. *https://doi.org/10.1016/j.saa.2010.12.079*